IFSCC 2025 full paper ***IFSCC2025-1834***

Screening for UVB/UVA absorbers in fungi associated with the macroalga *Phaeurus antarcticus* led to the isolation of photoprotective isocoumarins and a benzofuran with cosmeceutical applications

Gustavo Souza dos Santos 1 , Karen Cristina Rangel 1 , Izadora de Souza 1 , Ana Júlia Pasuch Gluzezak 1 , Ana Carolina Jordão 1 , Ludmila Tonanid 1 , Pio Colepicolo 2 , Marcia Regina von Zeska Kress 1 , Lorena Rigo Gaspar 1 , RuAngelie Edrada-Ebel 3 , Hosana Maria Debonsi 1 *

1 School of Pharmaceutical Sciences of Ribeirão Preto, University of São Paulo, Ribeirão Preto, Brazil; 2 Institute of Chemistry, University of São Paulo, São Paulo, Brazil; 3 Strathclyde Institute of Pharmacy and Biomedical Sciences, Strathclyde University, Glasgow, United Kingdom

1. Introduction

Antarctica is one of the most extreme environments on Earth, characterized by low temperatures, high UV radiation, low humidity, and seasonal light variation, resulting in ecosystems dominated by highly specialized marine organisms and microorganisms [1]. These harsh conditions drive the evolution of photoprotective mechanisms, including the production of secondary metabolites [2], which has encouraged the search for marine-derived compounds with cosmetic potential, such as anti-aging and UV-protective agents [3]. However, the growing demand for marine ingredients raises sustainability concerns, particularly regarding macroorganisms like algae. Cultivable marine microorganisms, especially fungi, offer a more sustainable alternative and have shown potential as sources of photoprotective and antioxidant compounds [4–7]. For instance, compounds from *Annulohypoxylon stygium* and *Exophiala* sp. demonstrated photostability and UVA protection superior to commercial UV filters [5,8]. Similarly, quinoline alkaloids from Antarctic *Penicillium echinulatum* showed UVA/UVB absorption, antioxidant activity, and photostability [7]. Given the harmful effects of UV radiation, including ROS production and DNA damage, and the toxicity of current sunscreens to both humans and marine life [6, 9], discovering safer and eco-friendly alternatives is essential. This study aimed to isolate endophytic fungi from the Antarctic macroalga *Phaeurus antarcticus* for the discovery of photoprotective compounds, using NMR and HRMS for chemical characterization and *in vitro* assays to evaluate bioactivity.

2. Materials and Methods

ISOLATION AND IDENTIFICATION OF ENDOPHYTIC FUNGI

Fungi were isolated from *P. antarcticus* samples collected from three islands in the South Shetland Archipelago: Halfmoon Island, Greenwich Island, and King George Island [10]. Fungal

identification was based on micromorphological analyses of vegetative development and asexual reproductive structures. Genomic DNA was extracted for molecular identification, followed by PCR amplification and sequencing of the ITS1 and ITS4 regions of ribosomal DNA [11].

INITIAL SCREENING OF EXTRACTS WITH UVB-UVA ABSORPTION

Cultivation and Extraction

Fungi were cultivated in four 500 mL Erlenmeyer flasks containing 150 mL of potato dextrose broth (also prepared in sterile seawater). Cultures were incubated statically at 24°C for 28 days. After this period, 150 mL of ethyl acetate was added to each flask. The biomass was separated by vacuum filtration, and the culture broth was extracted three times with ethyl acetate. The organic layer was concentrated under reduced pressure at a temperature not exceeding 35°C.

UVB-UVA Absorption and Photostability

Photodegradation of isolated metabolites was assessed by evaluating the absorption spectra (100 µg/mL solutions) of extracts, fractions, and isolated compounds using an Agilent 8453 spectrophotometer over a 200–400 nm range. Samples were irradiated or not with UVA light (4 mW/cm²) from a Philips UVA Actinic BL/10 lamp (Eindhoven, Netherlands) for 115 minutes, delivering a total dose of 27.6 kJ/cm². Photostability was determined by calculating the area under the curve (AUC) in the UVB (280–320 nm) and UVA (320–400 nm) ranges, as well as the UVA/UVB AUC ratio [12].

OSMAC-BASED OPTIMIZATION OF SECONDARY METABOLITE PRODUCTION

P. purpurogenum was cultivated in flasks containing 150 mL of medium. To optimize fermentation, two conditions were tested: I) potato dextrose broth in natural seawater (NSW), and II) potato dextrose broth in SW-BG11 (ASW). Cultures were incubated statically at 24°C. To assess changes in secondary metabolites, liquid-liquid extractions were performed on days 7, 14, and 21 for both media. Extracts were then analyzed for UVB-UVA absorption and photostability [12].

^{1}H NMR Analysis

Crude extracts of *P. purpurogenum* were prepared by dissolving each sample in 650 µL of DMSO-d6 (Sigma-Aldrich®) to a final concentration of 5 mg/mL. Proton NMR spectra were recorded on a Bruker® AVIII HD 400 spectrometer. Data were processed using MestReNova x64 version 14.1.2 (Mestrelab Research S.L.®) and submitted to multivariate statistical analysis. A heat map was constructed using the MetaboAnalyst platform (https://www.metaboanalyst.ca/).

SCALE-UP CULTIVATION, FRACTIONATION AND COMPOUND ISOLATION

P. purpurogenum was cultured in 60 flasks containing artificial seawater-based potato dextrose broth (CBD-ASW) for 14 days. The fermented broth was extracted with ethyl acetate and the crude extract (7.0 g) was subjected to vacuum liquid chromatography (VLC) on silica gel using a polarity gradient (hexane to methanol), yielding fractions FrE and FrF selected for further purification. FrE (350 mg) was fractionated on a Sep-Pak® silica column, producing 15 subfractions, with FrE-6 further purified by preparative RP-HPLC-DAD on a C8 column. FrF (600 mg) was fractionated via flash chromatography using a Biotage system, and subfraction FrF-4 was purified by preparative RP-HPLC-DAD under similar conditions.

PHOTOPROTECTIVE POTENTIAL EVALUATION

Photoprotection Against UVA Induced ROS Production in HaCaT Cells

Before the antioxidant assay, a cytotoxicity evaluation was conducted on HaCaT cells. Sodium dodecyl sulfate (SDS) was used as a positive control at 100 µg/mL. Cells were treated with the samples for 1 hour at 37°C under a 5% CO_2 atmosphere, and cell viability was assessed by the neutral red uptake (NRU) assay. All tests were performed in three independent experiments [13]. The production of intracellular ROS triggered by UVA irradiation was assessed using the $DCFH_2$-DA probe [14]. HaCaT cells were seeded in 96-well plates, incubated for 24 hours, washed with PBS, and treated with diluted samples for 1 hour. Compounds were tested at 50, 100, and 200 µg/mL. Quercetin and norfloxacin were used as ROS scavenger and generator controls at 10 and 100 µg/mL, respectively. After incubation, cells were washed twice and incubated with 10 µM $DCFH_2$-DA solution for 30 minutes. Plates were then washed, PBS was added to all wells, and plates were exposed to UVA radiation (Dr. Hönle solar simulator, SOL-500#, Planegg, Germany) at a dose of 4 J/cm². Fluorescence was immediately measured using a microplate reader with an excitation wavelength of 485 nm and an emission wavelength of 528 nm. Experiments were carried out in triplicate across three independent tests. The fluorescence of untreated irradiated cells was set at 100%, and the relative fluorescence of the samples was calculated accordingly.

Photoprotective Activity in the UVB Range

The UVB photoprotection assay was based on cell viability after exposure to a cytotoxic dose of UVB radiation. HaCaT cells were seeded in 96-well plates at a density of 1×10^5 cells/well and incubated for 24 h. Samples were diluted in PBS–Ca^{2+} at final concentrations of 200, 100, and 50 µg/mL for the test substance and 100 µg/mL for ethylhexyl methoxycinnamate (MTX). Plates were kept in the dark or irradiated with a UVB dose of 300 mJ/cm² (Philips Broadband UVB TL 40W/12 RS lamp), using an irradiance of 0.31 mW/cm² for 16 minutes. Non-irradiated untreated cells (NT – UV) and irradiated untreated cells (NT + UV) were used as negative and positive controls, respectively. Cell viability was evaluated using the NRU assay. Tests were carried out in triplicate across three independent experiments.

Photoprotection Against UVA-Induced ROS in Reconstructed Human Skin (RHS) Model

Dermal equivalents were constructed using primary fibroblasts, fetal bovine serum, and rat-tail type I collagen (3 mL per insert, six-well plate). After 2 hours, primary keratinocytes were seeded on top in 2 mL keratinocyte medium, kept submerged for 24 hours, and then maintained at the air-liquid interface for 12 days to promote differentiation. The detection of intracellular ROS in the RHS model using $DCFH_2$-DA (Sigma-Aldrich, St. Louis, MO, USA) was performed following the protocol [15]. Tissues were incubated with 50 µM $DCFH_2$-DA in the dark for 45 minutes, treated with compound 3 at 100 µg/mL (0.01% w/v), and irradiated with 10 J/cm² of UVA. Control tissues were kept in the dark. After irradiation, tissues were washed with PBS and cryopreserved in liquid nitrogen for 10 µm cryosectioning. Images were captured using an inverted Ti-S microscope (Nikon Instruments Inc., Netherlands) at 488 nm, with a 100 ms exposure. Fluorescence intensity was calculated and quantified using ImageJ software [16-17]. Results were expressed as percentage fluorescence relative to non-treated irradiated (+UV) and non-irradiated (-UV) controls, after fluorescence intensity normalization by area/pixel [15].

PHOTOSAFETY EVALUATION

Photoreactivity Studies – ROS Generation Assay

The ROS assay was performed to detect the generation of singlet oxygen and superoxide anion, following the ROS Assay Protocol Version 1.0 [18] and OECD Guideline 495 [19-21]. The generation of singlet oxygen ($^1O_2$, SO) was assessed by monitoring the bleaching of *p*-nitroso-*N*,*N*-dimethylalaniline (RNO) at 440 nm, using imidazole as a selective SO scavenger. The generation of superoxide anion (O_2^{-}•, SA) was evaluated by the reduction of nitroblue tetrazolium (NBT), followed by an increase in absorbance at 560 nm, according to the ROS Assay Protocol Version 1.0 [21]. The ROS assay was performed in triplicate across two independent runs. Octyl salicylate and histidine (20 µM) were used as negative and positive controls, respectively [19]. Octyl salicylate (20 µM) and quinine (200 µM) were used as negative and positive controls, respectively.

Phototoxicity Test in 3T3 Fibroblasts (3T3 NRU PT)

The isolated substances were subjected to the phototoxicity test based on neutral red uptake in murine 3T3 fibroblasts, following the OECD 432 guideline [21]. Norfloxacin was used as the positive control. One plate was exposed to a UVA irradiation dose of 9 J/cm², while the other plate was kept in the dark [22]. The assay was performed in triplicate across two independent experiments. Data were analyzed using the Phototox 2.0 software, which calculated the Mean Phototoxicity Effect (MPE).

HET-CAM Ocular Irritation Assay

Fertile Leghorn white chicken eggs (10th day of incubation) were used for the HET-CAM assay. The chorioallantoic membrane was exposed to compounds 3 and 4 (200 µg/mL). Sodium lauryl sulfate (1%) and sodium chloride (0.9%) were used as positive and negative controls, respectively. After 20 seconds of treatment, the membrane was washed, and irritation effects (hyperemia, hemorrhage, and coagulation) were observed for 5 minutes under a stereoscopic microscope. The irritation index was calculated based on the severity and appearance time of each effect. The test was performed in quadruplicate [23].

3. Results

Identification of Fungi and Screening of Extracts with Absorption in the UVB/UVA

Strains were identified as *Penicillium purpurogenum*, *Phaeoacremonium viticola*, *Cladosporium* sp., *Rhinocladiella simillis*, and *Epicoccum dendrobii*. The extract from *P. purpurogenum* presented the best absorption profile, mainly in the UVB (280-320 nm) and UVA II (320-340 nm) regions. In the photostability evaluation, all tested samples exhibited a photostable profile, except for the crude extract of *P. viticola*. The absorption spectra and photostability profiles are presented in Figure 1B and Table 1.

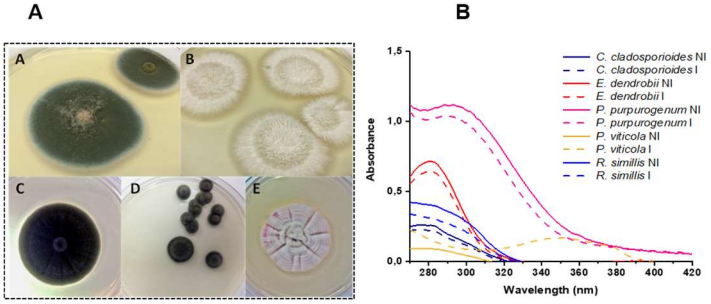

Figure 1. (A) Macromorphology of endophytic fungi isolated from the alga *Phaeurus antarcticus*. A) *P. purpurogenum*; B) *P. viticola*; C) *Cladosporium* sp.; D) *R. simillis*; E) *E. dendrobii*. (B) Absorption spectra

of crude extracts in the UVA-UVB range and photostability test based on the absorption spectrum after UVA irradiation (dashed line) or no irradiation (solid line).

Table 1. Remaining percentage of the area under the curve of irradiated samples compared to the non-irradiated samples, considered as 100%, in the UVA and UVB ranges.

Remaining absorption percentage relative to the non-irradiated pair (%)		
Extracts	**UVA**	**UVB**
Cladosporium sp.	-	83.7
E. dendrobii	-	87.0
P. purpurogenum	81.1	90.7
P. viticola	-	+ 241.0
R. simillis	-	73.9

P. purpurogenum was selected for a detailed investigation of its chemical profile and for the optimization of secondary metabolite production, aiming to isolate photoprotective compounds.

OPTIMIZATION OF SECONDARY METABOLITE PRODUCTION

Chemical Profile by ^{1}H NMR

NMR analysis revealed that secondary metabolite production varied with culture medium and incubation time. ASW-PDB extracts showed more peaks in the 11–12 and 8.5–9.5 ppm regions, associated with chelated hydroxyl-carbonyl groups, carboxylic acids, and aldehydes. Peak intensities also changed over time, with a noticeable decrease in the 21-day NSW-PDB extract. A heatmap analysis highlighted distinct chemical profiles: ASW-PDB extracts showed shifts toward aliphatic, aromatic, and deshielded proton regions over time, while NSW-PDB extracts displayed more diverse and time-dependent signals, indicating media- and time-specific chemical diversity.

Absorption in the UVB/UVA Range and Photostability

The results of the UV absorption profile (Figures 2A and 2B) showed that, for both media, the 14-day incubation resulted in higher absorption. For this reason, both 14-day crude extracts were subjected to the photostability test. When compared to the non-irradiated counterparts, the 14-day NSW extract retained 78.7% of its absorbance in the UVB range and 60.9% in the UVA- range (Fig. 2). The 14-day ASW extract, on the other hand, retained 90.4% of its absorbance in the UVB range and 85.2% in the UVA.

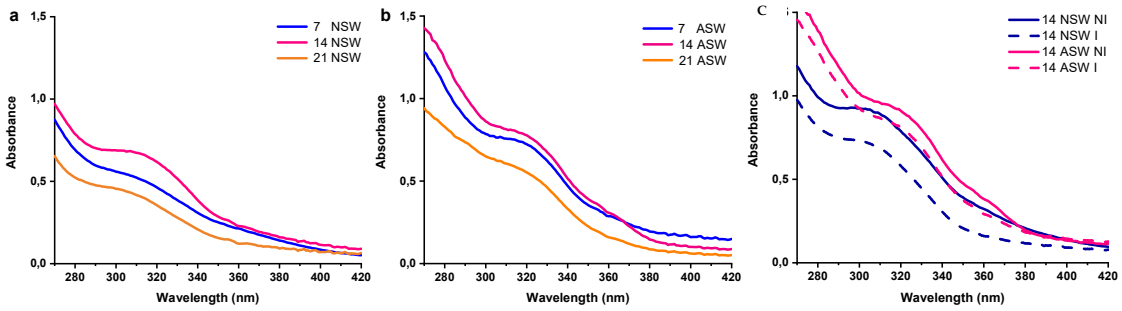

Figure 2. Absorption spectra of *P. purpurogenum* extracts in the UVA/UVB region. (A) Crude extracts from PDB-NSW medium; (B) Crude extracts from PDB-ASW medium; (C) photostability assay based on the absorption spectra after UVA irradiation (dotted line) or not (solid line) of the 14-day NSW and 14-day ASW crude extracts.

PHOTOPROTECTIVE POTENTIAL OF COMPOUNDS ISOLATED FROM *P. purpurogenum*

Two compounds (**1–2**) were isolated from fraction FrE, and two compounds (**3–4**) from fraction FrF. The isolated metabolites belong to the isocoumarin and benzofuran classes.

UVB/UVA Absorption and Photostability

Fractions FrE and FrF showed promising absorption profiles and were considered photostable (Figure 3). Since most commercial sunscreens contain only UVB-absorbing filters, this absorption profile is particularly interesting. Compounds **1–4** were isolated and evaluated for their absorption profile and photostability. Compounds were considered photostable, with remaining absorption spectra greater than 80% (Table 2, Figure 4).

Table 2. Remaining percentage of the area under the curve of irradiated samples compared to non-irradiated samples, considered as 100%, in the UVA and UVB ranges.

Percentage of remaining absorption relative to the non-irradiated pair (%).		
Samples	**UVA**	**UVB**
FrE	81.8	94.2
FrF	80.2	89.2
(**1**)	95.6	89.5
(**2**)	85.3	93.7
(**3**)	+ 17.5	+ 25.1
(**4**)	-	+ 34.4

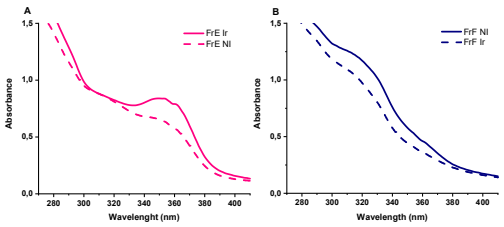

Figure 3. Absorption spectra in the UVA-UVB region and photostability assay based on the absorption spectrum after UVA irradiation (dashed line) or not (solid line). A – Fraction E; B – Fraction F.

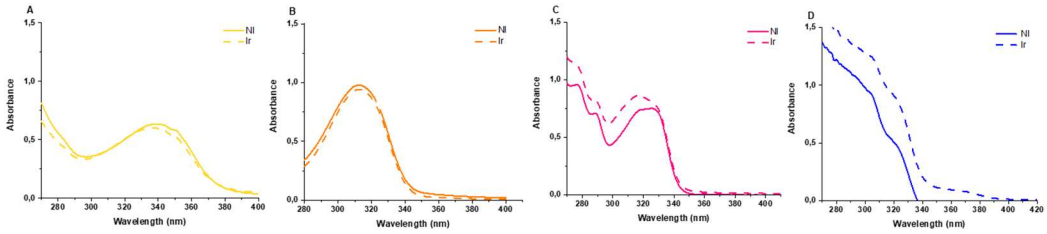

Figure 4. Absorption spectra in the UVA/UVB region and photostability assay based on the absorption spectrum after UVA irradiation (dashed line) or not (solid line). A – Compound (**1**); B – Compound (**2**); C – Compound (**3**); D – Compound (**4**). Compounds (**1**–**2**) were isolated from fraction FrE, and compounds (**3**–**4**) from fraction FrF.

Photoprotective Activity Against UVB

Compounds (**2-4**) were evaluated for UVB photoprotection in a cell viability assay, with ethylhexyl-methoxycinnamate (MTX) used as a commercial filter for comparison. Compound (**2**) maintained 96% viability at 200 µg/mL and 64% at 100 µg/mL. Compound (**4**) exhibited the highest photoprotection, preserving 100% viability at 200 µg/mL and 94% at 100 µg/mL. Compound (**3**) also demonstrated UVB protection, with cell viability at 79% (200 µg/mL) and 59% (100 µg/mL). Untreated controls showed 32% viability, while MTX-treated cells had 67% viability at both concentrations.

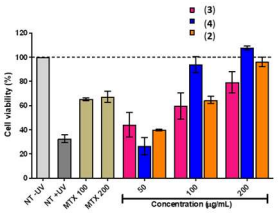

Figure 5. Viability of HaCaT cells after treatment with the isolated compounds (200, 100, and 50 µg/mL) and ethylhexyl methoxycinnamate (MTX; 100 and 200 µg/mL) followed by UVB irradiation (300 mJ/cm²). Untreated and non-irradiated (NT – UV); untreated and irradiated (NT + UV). Results are expressed as mean ± SEM (n = 3).

Photoprotection Against UVA Induced ROS Production in HaCaT Cells

Before the photoprotection assay, a cytotoxicity evaluation was conducted on HaCaT cells. As shown in Figure 6A, none of the compounds exhibited cytotoxicity at the tested concentrations (50-200 µg/mL). In the antioxidant assay, the results revealed that only compound **3** was able to protect the cell from UVA by 15% at all tested concentrations (200 - 50 µg/mL) (Figure 6B).

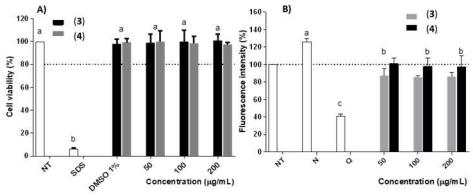

Figure 6. A) Preliminary cytotoxicity in HaCaT cells. B) Quantification of intracellular ROS induced by UVA radiation in HaCaT cells after pre-treatment with the test samples for 1 hour. The results are expressed as % fluorescence. The cells were either untreated and irradiated (+UV) or non-irradiated (−UV) and pre-treated with quercetin (Q: 10 µg/mL), norfloxacin (N: 100 µg/mL), compounds (**3**) and (**4**) (200, 100, and 50 µg/mL).

Photoprotection Against UVA-Induced ROS Production in RHS

According to the results, compound (**3**) was able to protect the skin models (RHS) from UVA-, reducing ROS production by 30% compared to the untreated control (Fig. 7).

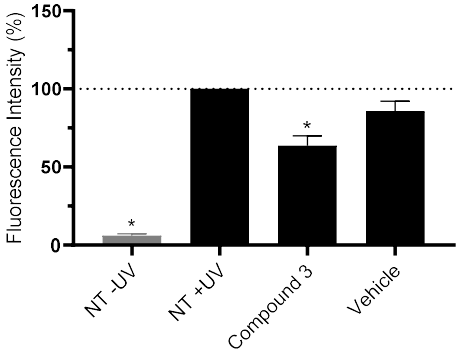

Figure 7. ROS quantification induced by UVA radiation in the RHS model, results expressed as % of pixels/area of fluorescence intensity. The skin models were untreated and non-irradiated (NT UV-) and untreated and irradiated (NT UV+), compound **3** at 200 µg/ml in sesame oil (vehicle) (0.02% p/v) and irradiated with vehicle only.

PHOTOTOSAFETY EVALUATION

Photoreactivity Study – ROS Generation Assay

The photoreactivity potential of the compounds was evaluated by irradiating the samples followed by the measurement of ROS: singlet oxygen (SO) and superoxide anion (SA). All compounds were considered non-photoreactive (Table 3).

Table 3. Photoreactivity assay of compounds **2–4**. Results are expressed as mean ± standard deviation from two independent experiments.

Amostra	SO (ΔA_{440nm} x 10^3)	SA (ΔA_{560nm} x 10^3)	Results*
Quinine (CP+)	543.50 ± 13.64	336.60 ± 52.87	Photoreactive
Ketoprofen (CP+)	316.95	101.03	Photoreactive
Octyl salicylate (CN−)	4.46 ± 8.41	-15.73 ± 1.31	Non-photoreactive
Histidine (CN−)	- 1.4	17.48	Non-photoreactive
(**2**)	4.76 ± 6.74	-9.10 ± 6.44	Non-photoreactive
(**3**)	4.05	12.73	Non-photoreactive
(**4**)	0.58	14.43	Non-photoreactive

*Photoreactive: SO ≥ 25 and SA ≥ 70, and non-photoreactive: SO < 25 and SA < 20.

3T3 NRU Phototoxicity Test (3T3 NRU PT)

Norfloxacin was classified as phototoxic, with an MPE value within the range recommended by OECD Guideline 432 [26]. Compounds were considered non-cytotoxic, as the IC_{50} of the non-irradiated samples (UV–) was greater than the tested range (100 µg/mL). Regarding phototoxicity, only compound (**3**) was classified as non-phototoxic. The results are summarized in Table 4.

Table 4. Phototoxicity assay in BALB/c 3T3 fibroblasts expressed as MPE values for compounds **1**–**4** and the positive control (norfloxacin) from two independent experiments.

Sample	Ensaio	MPE	IC_{50} (-UV) µg mL^{-1}	IC_{50} (+UV) µg mL^{-1}	Resultado

(**1**)	1	0.303	ND	34.09	Phototoxic
	2	0.157	ND	24.50	Non-cytotoxic
(**2**)	1	0.431	ND	13.43	Phototoxic
	2	0.458	ND	15.77	Non-cytotoxic
(**3**)	1	- 0.031	ND	> 100	Non-phototoxic
	2	0.071	ND	> 100	Non-cytotoxic
(**4**)	1	0.327	ND	57.21	Phototoxic
	2	0.307	ND	64.15	Non-cytotoxic
Norfloxacina	1	0.654	ND	28.88	Phototoxic
	2	0.507	ND	49.53	Non-cytotoxic

HET-CAM eye irritation test

The compounds (**3**) and (**4**) received scores of (0±0) and were classified as non-irritants due to the absence of coagulation, hemorrhage, and hyperemia effects. The results for compounds (**3**) and (**4**) are summarized in Table 5.

Table 5. Irritation score, reported as mean ± standard error of the mean (n = 4), and classification of the effects of the compounds in the HET-CAM assay. Sodium lauryl sulfate (SDS) and sodium chloride (NaCl) solutions were used as positive and negative controls, respectively.

Sample	Mean score ± SD	Classification
NaCl 0.9%	0 ± 0	Non-irritant
SDS 1%	12 ± 0	Severe irritant
Vehicle (DMSO 1%)	0 ± 0	Non-irritant
(**3**)	0 ± 0	Non-irritant
(**4**)	0 ± 0	Non-irritant

4. Discussion

Coumarins are widely used in the treatment of skin conditions such as psoriasis and vitiligo and are common in cosmetic fragrances due to their photoprotective and antioxidant properties [24]. Isocoumarins, such as hydroxymellein from *P. austrosinense*, have shown antioxidant activity and promoted HaCaT cell recovery after UVB exposure [25]. Despite their potential, fungal metabolites remain underexplored as photoprotective agents. Regarding photoprotection against ROS induced by UVA irradiation, for both models compound 3 showed antioxidant potential. Differences in ROS inhibition between HaCaT monolayers and RHS models may result from the stratum corneum limiting compound penetration. Enhancing formulations with surfactants and penetration enhancers could improve bioavailability without causing photoirritation [26]. Similar outcomes were reported for quinoline alkaloids from *P. echinulatum*, which demonstrated stronger antioxidant activity in RHS [6]. Moreover, the monolayer model is limited and fails to replicate the complexity of living tissue, unlike the reconstructed human skin (RHS) model, which engages more effectively with the skin's natural antioxidant mechanisms**.** Photoreactivity is critical when evaluating UV filters, as ROS generation can lead to oxidative damage

and photoaging [27]. Our findings support the potential of the compounds as non-photoreactive ingredients. The 3T3 NRU assay is a standard method for phototoxicity screening; however, positive results require further testing due to its susceptibility to false positives [28]. The RHS model, which mimics human skin's barrier, is more predictive of *in vivo* bioavailability [15]. Viridicatine and viridicatol, isolated from *P. echinulatum*, absorbed UVB and UVA-II radiation and were non-phototoxic in RHS, despite positive results in 3T3 NRU [6]. Concerns over animal testing have driven the adoption of alternative methods. The HET-CAM assay, an alternative to the Draize test, evaluates ocular irritation using the chorioallantoic membrane of chicken eggs [29]. This method has been used to assess irritation from plant extracts [30], mycosporine-rich algae [31], and polyketides from Antarctic fungi [32]. These alternative models are vital for ensuring the safety and efficacy of natural compounds in cosmetic and pharmaceutical applications.

5. Conclusion

This study highlights the Antarctic seaweed *P. antarcticus* as a reservoir of endophytic fungi, capable of producing photoprotective secondary metabolites. Through a combination of fungal isolation, molecular identification, OSMAC-based optimization, and bioguided fractionation, four compounds were isolated from *P. purpurogenum*. The comprehensive *in vitro* assessment demonstrated that these compounds exhibit promising UV absorption profiles, photostability, and protective effects against UV-induced cytotoxicity and oxidative stress in skin models. Compound (**3**) stood out due to its potent photoprotective and antioxidant activities, combined with a safe profile in our evaluation, reinforcing its potential as a candidate for development in topical sunscreen formulations. These findings contribute to the ongoing search for sustainable, marine-derived photoprotective agents.

7. References

1. dos Santos GS, et al. Natural products from the poles: structural diversity and biological activities. Rev Bras Farmacogn. 2021;31(5):531-60.
2. Núñez-Pons L, et al. UV-protective compounds in marine organisms from the Southern Ocean. Mar Drugs. 2018;16(9):336.
3. Agrawal S, Adholeya A, Barrow CJ, Deshmukh SK. Marine fungi: An untapped bioresource for future cosmeceuticals. Phytochem Lett. 2018;23:15-20.
4. Maciel OMC, Tavares RSN, Caluz DRE, Gaspar LR, Debonsi HM. Photoprotective potential of metabolites isolated from algae-associated fungi *Annulohypoxylon stygium*. J Photochem Photobiol
5. Pallela R, Na-Young Y, Kim SK. Anti-photoaging and photoprotective compounds derived from marine organisms. Mar Drugs. 2010;8(4):1189-202.
6. Teixeira TR, et al. In vitro evaluation of the photoprotective potential of quinolinic alkaloids isolated from the Antarctic marine fungus *P. echinulatum* for topical use. Mar Biotechnol. 2021;23:357-72.
7. Zhang D, Yang X, Kang JS, Choi HD, Son BW. Circumdatin I, a new ultraviolet-A protecting benzodiazepine alkaloid from a marine isolate of the fungus *Exophiala*. J Antibiot. 2008;61(1):40-2.
8. Pfeifer GP. Mechanisms of UV-induced mutations and skin cancer. Genome Instab Dis. 2020;1(3):99-113.
9. Jesus A, et al. UV filters: challenges and prospects. Pharmaceuticals. 2022;15(3):263.
10. Teixeira TR, et al. Characterization of the lipid profile of Antarctic brown seaweeds and their endophytic fungi by gas chromatography–mass spectrometry (GC–MS). Polar Biol. 2019;42:1431-44.
11. White TJ, et al. Amplification and direct sequencing of fungal ribosomal RNA genes for phylogenetics. PCR Protocols. 1990;18(1):315-22.
12. Gaspar LR, Campos PM. Evaluation of the photostability of different UV filter combinations in a sunscreen. Int J Pharm. 2006;307(2):123-8.
13. Repetto G, Del Peso A, Zurita JL. Neutral red uptake assay for the estimation of cell viability/cytotoxicity. Nat Protoc. 2008;3(7):1125-31.
14. Kalyanaraman B, et al. Measuring reactive oxygen and nitrogen species with fluorescent probes: challenges and limitations. Free Radic Biol Med. 2012;52(1):1-6.
15. Tavares RSN, et al. Fucoxanthin for topical administration, a phototoxic vs. photoprotective potential in a tiered strategy assessed by in vitro methods. Antioxidants. 2020;9(4):328.
16. Rasmussen C, et al. The StrataTest® human skin model, a consistent in vitro alternative for toxicological testing. Toxicol In Vitro. 2010;24(7):2021-9.
17. Marionnet C, et al. Diversity of biological effects induced by longwave UVA rays (UVA1) in reconstructed skin. PLoS One. 2014;9(8):e105263.
18. OECD. OECD guidelines for testing of chemicals, Test No. 495: ROS Assay for Photoreactivity. 2019a. Available from: https://www.oecd-ilibrary.org/docserver/915e00acen.pdf
19. ICH. ICH Harmonized tripartite Guideline: Photosafety Evaluation of Pharmaceuticals S10. 2013. Available from: https://database.ich.org/sites/default/files/S10_Guideline.pdf

20. Onoue S, et al. Establishment and intra-/inter-laboratory validation of a standard protocol of ROS assay for chemical photosafety evaluation. J Appl Toxicol. 2013;33(11):1241-50.

21. OECD. OECD guidelines for testing of chemicals, Test No. 432: In vitro 3T3 NRU Phototoxicity Test. 2019b.

22. Gaspar LR, et al. Skin phototoxicity of cosmetic formulations containing photounstable and photostable UV-filters and vitamin A palmitate. Toxicol In Vitro. 2013;27(1):418-25.

23. de Lima Sá L, et al. Strategies for the evaluation of the eye irritation potential of different types of surfactants and silicones used in cosmetic products. Toxicol In Vitro. 2022;81:105351.

24. Kasperkiewicz K. Sunscreening and photosensitizing properties of coumarins and their derivatives. Lett Drug Des Discov. 2016;13(5):465-74.

25. Zhao L, et al. A multifunctional and possible skin UV protectant, (3R)-5-hydroxymellein, produced by an endolichenic fungus isolated from Parmotrema austrosinense. Molecules. 2016;22(1):26.

26. Pivetta TP, et al. Topical formulation of quercetin encapsulated in natural lipid nanocarriers: Evaluation of biological properties and phototoxic effect. J Drug Deliv Sci Technol. 2019;53:101148.

27. Buchalska M, et al. Singlet oxygen generation in the presence of titanium dioxide materials used as sunscreens in suntan lotions. J Photochem Photobiol A. 2010;213(2-3):158-63.

28. Kejlová K, et al. Phototoxicity of bergamot oil assessed by in vitro techniques in combination with human patch tests. Toxicol In Vitro. 2007;21(7):1298-303.

29. Luepke NP, Kemper FH. The HET-CAM test: an alternative to the Draize eye test. Food Chem Toxicol. 1986;24(6-7):495-6.

30. Thiesen LC, et al. Photochemoprotective effects against UVA and UVB irradiation and photosafety assessment of Litchi chinensis leaves extract. J Photochem Photobiol B. 2017;167:200-7.

31. Rangel KC, et al. Assessment of the photoprotective potential and toxicity of Antarctic red macroalgae extracts from Curdiea racovitzae and Iridaea cordata for cosmetic use. Algal Res. 2020;50:

32. Jordão AC, et al. Assessment of the photoprotective potential and structural characterization of secondary metabolites of Antarctic fungus Arthrinium sp. Arch Microbiol. 2024;206(1):35.